Geographic, seasonal, and precipitation chemistry influence on the abundance and activity of biological ice nucleators in rain and snow

Brent C. Christner[a,1], Rongman Cai[b,2], Cindy E. Morris[c], Kevin S. McCarter[b], Christine M. Foreman[d,e], Mark L. Skidmore[f], Scott N. Montross[f], and David C. Sands[g]

Departments of [a]Biological Sciences and [b]Experimental Statistics, Louisiana State University, Baton Rouge, LA 70803; [c]Unité de Pathologie Végétale UR407, Institut National de la Recherche Agronomique, F-84140 Montfavet, France; and [d]Center for Biofilm Engineering and Departments of [e]Land Resources and Environmental Sciences, [f]Earth Sciences, and [g]Plant Sciences and Plant Pathology, Montana State University, Bozeman, MT 59717

Communicated by P. Buford Price, Jr., University of California, Berkeley, CA, October 7, 2008 (received for review August 14, 2008)

Biological ice nucleators (IN) function as catalysts for freezing at relatively warm temperatures (warmer than −10 °C). We examined the concentration (per volume of liquid) and nature of IN in precipitation collected from Montana and Louisiana, the Alps and Pyrenees (France), Ross Island (Antarctica), and Yukon (Canada). The temperature of detectable ice-nucleating activity for more than half of the samples was ≥ −5 °C based on immersion freezing testing. Digestion of the samples with lysozyme (i.e., to hydrolyze bacterial cell walls) led to reductions in the frequency of freezing (0–100%); heat treatment greatly reduced (95% average) or completely eliminated ice nucleation at the measured conditions in every sample. These behaviors were consistent with the activity being bacterial and/or proteinaceous in origin. Statistical analysis revealed seasonal similarities between warm-temperature ice-nucleating activities in snow samples collected over 7 months in Montana. Multiple regression was used to construct models with biogeochemical data [major ions, total organic carbon (TOC), particle, and cell concentration] that were accurate in predicting the concentration of microbial cells and biological IN in precipitation based on the concentration of TOC, Ca^{2+}, and NH_4^+, or TOC, cells, Ca^{2+}, NH_4^+, K^+, PO_4^{3-}, SO_4^{2-}, Cl^-, and HCO_3^-. Our results indicate that biological IN are ubiquitous in precipitation and that for some geographic locations the activity and concentration of these particles is related to the season and precipitation chemistry. Thus, our research suggests that biological IN are widespread in the atmosphere and may affect meteorological processes that lead to precipitation.

atmosphere | climate | microbial dissemination | biological ice nuclei

At subzero temperatures warmer than −40 °C, aerosol particles in clouds initiate freezing through the heterogeneous nucleation of ice directly from water vapor or by freezing droplets via several mechanisms: deposition, condensation, contact, and immersion freezing (1). These processes lead to ice formation in clouds that can trigger precipitation. A diverse range of natural and anthropogenic particles, referred to as ice-forming nuclei or ice nucleators (IN), are capable of initiating the ice phase (2). The maximum temperature at which an IN can initiate freezing is specific to that nucleator, but they function similarly by providing templates for the aggregation of individual water molecules in the configuration of an ice embryo, resulting in a subsequent phase change and the cascade of crystal formation (3). Consequently, knowledge of the nature and sources of IN in the atmosphere is important for understanding the meteorological processes responsible for precipitation. The most active naturally occurring IN are biological in origin and have the capacity to catalyze freezing at temperatures near −2 °C (4). The most widespread and well-studied biological aerosols with ice-nucleating activity are comprised of certain species of plant-associated bacteria (*Pseudomonas syringae, Pseudomonas viridiflava, Pseudomonas fluorescens, Pantoea agglomerans,* and *Xanthomonas campestris*), but also fungi (e.g., *Fusarium avenaceum*), algae such as *Chlorella minutissima,* and birch pollen (5). *P. syringae* (6–8) and *F. avenaceum* (7) in particular have been detected in atmospheric aerosols and clouds. Ice-nucleating strains of *P. syringae* possess a 120- to 180-kDa ice nucleation active protein in their outer membrane comprised of contiguous repeats of a consensus octapeptide; the protein binds water molecules in an ordered arrangement, providing a nucleating template that enhances ice crystal formation (9).

Based on reports of ice-nucleating bacteria at altitudes of several kilometers (6, 10) and the warm temperatures at which they function as ice nuclei (−2 °C to −7 °C; ref. 5), biological IN may play a role in the precipitation cycle. Very large numbers of microorganisms inhabit leaf surfaces globally (10^{24} to 10^{26} cells; ref. 11), deciduous plants harbor large populations of ice-nucleating bacteria on their leaves (≈10^5 ice-nucleating bacteria cm^{-2}; ref. 12), and various species of ice-nucleating bacteria or biological IN in general have been detected in phytoplankton-rich marine waters (13), snow (14, 15), and rain (15, 16). Although biological particles represent a significant component of atmospheric aerosols (17), few data have been available on the concentration of airborne biological ice nuclei. Therefore, the abundance and distribution of the most active IN in the atmosphere (i.e., biological IN) are described in only a very limited way and their meteorological role is unknown.

Our previous work on snowfall collected from a variety of mid- and high-latitude locations indicated that biological IN are ubiquitous in precipitation from a range of global locations and represent the most active IN at temperatures warmer than −10 °C (14). Here, we present results from a comprehensive analysis of biological IN in snow and rain and use statistical methods to examine correlations between the microbiological and biogeochemical data. A primary objective of this study was to elucidate biogeochemical markers of the presence of biological IN to provide information on conditions that favor their distribution in the atmosphere and predict other contexts where they would be abundant. We show that for some geographical locations the concentration (i.e., per rain or snow water equivalent volume) and activity of biological IN is correlated with the biogeochemistry of the precipitation and season of deposition.

Author contributions: B.C.C., C.E.M., and D.C.S. designed research; B.C.C., R.C., and C.E.M. performed research; C.M.F., M.L.S., and S.N.M. contributed new reagents/analytic tools; B.C.C., R.C., and K.S.M. analyzed data; and B.C.C. wrote the paper.

The authors declare no conflict of interest.

[1]To whom correspondence should be addressed. E-mail: xner@lsu.edu.

[2]Present address: Department of Plant Pathology, Virginia Polytechnic Institute and State University, Blacksburg, VA 24061.

This article contains supporting information online at www.pnas.org/cgi/content/full/0809816105/DCSupplemental.

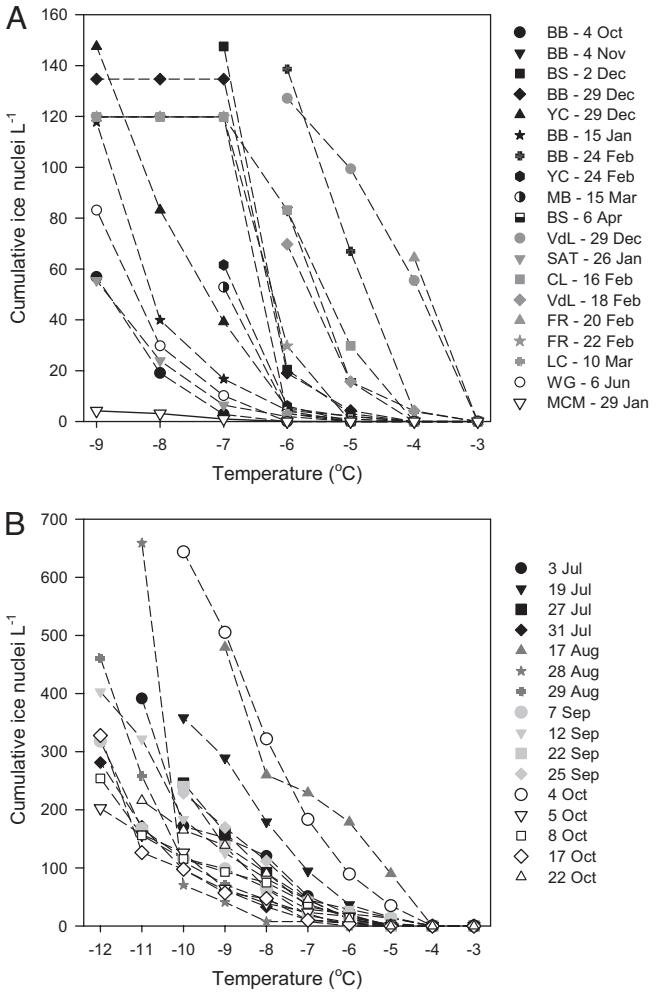

Fig. 1. The cumulative ice nuclei spectra for particles >0.22 μm in snow samples collected from Montana, France, Yukon, and Antarctica (*A*) and rain samples from Louisiana (*B*). Site designations are Bridger Bowl, Montana (BB); Big Sky, Montana (BS); The Yellowstone Club, Montana (YC); Moonlight Basin, Montana, (MB); McMurdo Station, Antarctic (MCM); Wheaton Glacier, Yukon (WG); La Clusaz, France (CL); Villard de Lans, France (VdL); Saint-Françoise Longchamp, France (LC); Font Romeu, France (FR); and St. Saturnin-les-Avignon, France (SAT).

Results

Warm Temperature IN in Snow and Rain. The cumulative spectra of IN per unit volume of snow water detected at temperatures ≥ -9 °C in 19 snow samples from sites in Montana, France, Antarctica, and the Yukon Territory from October 2005 to June 2006 and ≥ -12 °C in 16 Louisiana rain samples from July to October 2007 are shown in Fig. 1. The samples for immersion freezing testing of rain were reconstituted in deionized water at a lower concentration factor than similar particle suspensions from the snow samples, and therefore, the latter contained 5- to 10-fold fewer total IN per unit volume tested. This difference allowed the IN concentration in rain to be determined at temperatures as low as -12 °C, whereas aliquots of the particle-concentrated solutions from the snow samples were typically frozen by -9 °C. We refer to these IN as "ice nuclei," consistent with the terminology used in the atmospheric sciences (1).

At temperatures warmer than -10 °C, the lowest concentrations of ice nuclei in snow (4 ice nuclei L^{-1} of melt water) were observed in samples from Antarctica (Fig. 1*A*) and highest measurable concentrations were in samples from Montana (150 ice nuclei L^{-1}). Calculation of the ice nuclei concentration at a given temperature using immersion freezing testing requires that at least one aliquot tested remains unfrozen. For this reason, it was not possible to determine the ice nuclei concentration over the entire experimental temperature range tested for all samples. Given that the cumulative concentration of ice nuclei typically increases with decreasing temperature, samples where all aliquots were frozen at the warmer temperatures assayed probably contained much higher ice nuclei concentrations at -9 °C than the upper limit values we report. In general, snow samples from France contained higher concentrations of ice nuclei that were active at warmer temperatures relative to those in samples from Montana and higher latitudes.

In rain samples from Louisiana, the lowest and highest ice nuclei concentrations at temperatures warmer than -10 °C (41 and 510 ice nuclei L^{-1}, respectively) were observed in samples collected in August and October, respectively (Fig. 1*B*). Comparison of the cumulative ice nuclei concentration spectra in rain collected from July through October 2007 revealed variation among the samples, with differences ranging by a factor of 12 to 180 at temperatures between -5 °C and -9 °C. There were clearly 2 outlying samples (August 17 and October 4) that contained significantly higher ice nuclei concentrations at -9 °C (480 and 510 ice nuclei L^{-1}, respectively) than the other rainfalls analyzed. However, the highest measurable ice nuclei concentration was observed at -11 °C (660 ice nuclei L^{-1}) from a sample collected on August 28 in which the ice nuclei concentration increased nearly 10-fold between -10 °C and -11 °C (Fig. 1*B*). When the cumulative ice nuclei concentration at temperatures warmer than -7 °C in snow from various locations (Fig. 1*A*) is compared with that in rain from Louisiana (Fig. 1*B*), the range of ice nuclei concentrations observed was similar (1–150 ice nuclei L^{-1} in snow; 8–230 ice nuclei L^{-1} in rain).

Biological Ice Nuclei in Precipitation. Most known biological ice nuclei are efficient at catalyzing freezing because of the presence of proteinaceous IN (5). Therefore, the concentration of ice nuclei that were sensitive to heat (i.e., to disrupt the structure of proteinaceous IN) was inferred to represent the total pool of biological ice nuclei in a sample (hereafter referred to as the total biological ice nuclei fraction). Furthermore, few other naturally occurring particles in the atmosphere have nucleating temperatures as warm as those of biological ice nuclei and would not be expected to have any noticeable change in activity, caused by the heat treatment, at the temperatures of our freezing tests. Although the coefficient of variation was high for data collected at a given geographical location (0.6–0.8), snow samples from France and Montana contained a similar average concentration of biological ice nuclei active at ≥ -9 °C (55 and 54 ice nuclei L^{-1}, respectively) compared with higher values for Louisiana rain (110 ice nuclei L^{-1}; calculated excluding data outliers from August 17 and October 4; Fig. 1*B*) [supporting information (SI) Fig. S1], but these differences were statistically significant only between the Montana and Louisiana samples ($P = 0.04$).

Heat treatment completely eliminated ice nucleation at temperatures ≥ -9 °C in 69–100% of the snow and rain samples. Lysozyme catalyzes the hydrolysis of peptidoglycan molecules in bacterial cell walls thereby destabilizing their ability to maintain tertiary structure of the IN proteins, which is important for their activity as IN. Lysozyme-sensitive bacteria represented the majority of ice nuclei at ≥ -9 °C in 64%, 50%, and 25% of the samples from France, Montana, and Louisiana, respectively (Fig. 2). Although there was little variation between samples and locations in the fraction of total ice nuclei active at ≥ -9 °C that were sensitive to heat (>92%), there were substantial differences in the percentage of ice nuclei that were susceptible to lysozyme (0–100%) and maximum temperature of ice-nucleating activity (-4 °C to -7 °C) (Fig. 2 and Fig. S1). The

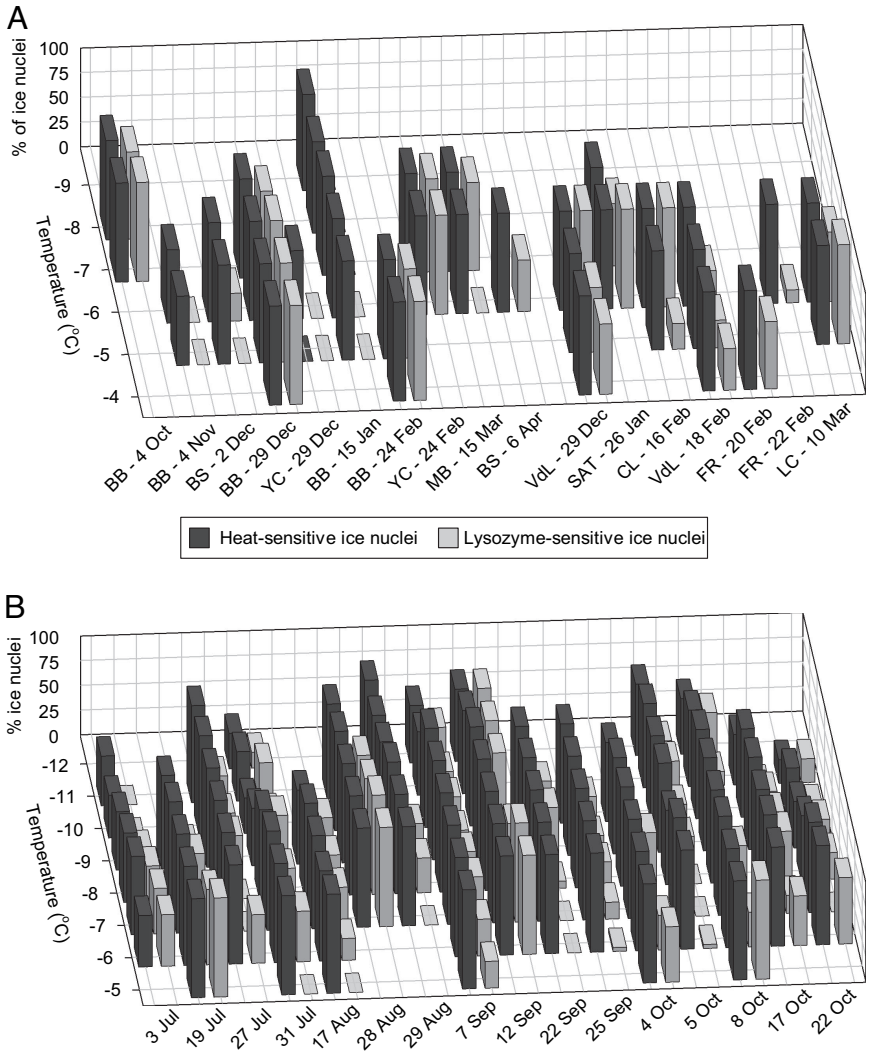

Fig. 2. The percentage of ice nuclei at decreasing temperature that were susceptible to heat treatment and lysozyme digestion. (*A*) Snow from Montana and France. (*B*) Rain from Louisiana. See Fig. 1 legend for site designations.

average proportion of heat-sensitive ice nuclei that were inactivated by lysozyme was slightly higher in samples from France (63%) compared with those from Montana (51%) and Louisiana (36%). At temperatures between −10 °C and −12 °C, the average percentage of ice nuclei that were heat-sensitive (63–83%) and lysozyme-sensitive (24–30%) in Louisiana rain generally decreased with temperature (Fig. 2*B*). Despite an overall decreasing trend with temperature, the highest concentrations of biological (630 ice nuclei L^{-1} at −11 °C, 95% of the total; August 28) and bacterial (290 ice nuclei L^{-1} at −12 °C, 73% of the total; September 12) ice nuclei were observed at temperatures below −10 °C in Louisiana rain samples (Fig. 2*B* and Fig. S1*B*). Two fresh snow samples were analyzed from Antarctica and Yukon, and all of the ice nuclei active at ≥ −9 °C were susceptible to the heat treatment, whereas 0–100% and 35–56%, respectively, of these ice nuclei were destroyed by lysozyme (data not shown). When the precipitation data from the various global locations are compiled, the average percent of ice nuclei active at ≥ −9 °C that were inactivated by lysozyme and the heat treatment was 42% and 95%, respectively.

There were certain precipitation events in the Montana (BB, October 4, December 29, and February 24; YC, February 24; and BS, April 6), France (VdL, December 29; SAT, January 26; LC, March 10), and Louisiana (August 28 and September 12) samples in which bacteria dominated the fraction of ice nuclei active at all temperatures warmer than −9 °C (52–100% of the total; Fig. 2). Three samples from Montana (BB, November 4 and January 15; YC, December 29) contained 4–110 biological ice nuclei L^{-1} that were active at > −9 °C (Fig. S1*A*), but none of these ice nuclei were sensitive to lysozyme. There were 2 dates in the Montana snow record (December 29 and February 24) where samples were collected at different sites ≈80 km apart (Fig. 2*A*), and there were significant differences in the concentration of all classes of ice nuclei between sites. In particular, 95% confidence interval estimates of the cumulative concentrations at −7 °C (BB and YC sites on December 29 are [69.1, 281.8] and [24.5, 59.3], respectively; [72.8, 285.7] and [1.6, 15.8] for February 24, respectively) do not overlap, providing strong evidence that the cumulative concentrations at the two sites were significantly different.

Cluster Analysis of Montana Snowfall. To investigate similarities between snow events in terms of the ice nuclei active at ≥ −9 °C, cluster analysis was used to organize the snow events into groups having similar freeze profiles (Fig. 3). The cumulative ice nuclei concentration at a given temperature is a monotone function of the probability of being frozen at that temperature. This finding implies that snow events that are similar with respect to the

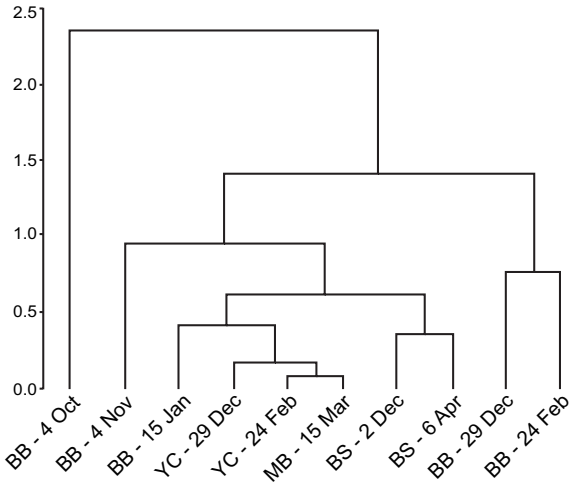

Fig. 3. Cluster analysis of Montana snowfall by the complete linkage method. The scale bar indicates the maximum distance between clusters. Each sample is designated by the site of collection (see Fig. 1 legend for site designations) and the date of precipitation.

cumulative ice nuclei concentration will be similar with respect to their freeze profiles as well, so that assessments of similarity based on these two quantities will be essentially equivalent. This idea was verified empirically by comparing curves generated from the freeze probabilities (data not shown) with those of the estimated cumulative ice nuclei spectra (Fig. 1), which showed that the shapes of the freeze profiles matched those of the ice nuclei content in the corresponding snow samples.

The single-linkage, complete-linkage, average-linkage, and Ward's method produced dendrograms with slightly different topologies (Fig. 3 and Fig. S2). That these methods have produced somewhat different results is not unusual or unexpected. Because the four methods apply different metrics, they use different aspects of the data in forming clusters, and consequently, can produce different results in general. However, all four methods agree in several ways: (*i*) the October and November snow events from the BB site appear to be different from the other observations and are grouped separately; (*ii*) the BB December 29 and February 24 snow events are always clustered and are not similar to samples collected on the same date from the YC site; and (*iii*) snow events from the BB site were always grouped separately from those collected from sites that are <10 km apart (i.e., the BS, YC, and MB sites).

Statistical Modeling of the Cell and Biological Ice Nuclei Concentrations in Snow. The major ion, total organic carbon (TOC), particle, cell (Table S1), and biological ice nuclei (where applicable) concentration data from the Montana snow record (Fig. S1*A*) were used to construct multiple regression models in SAS. Because of the small sample size ($n = 10$) and the comparatively large number of explanatory variables ($P = 14$ or 15), model selection procedures that consider subsets of the explanatory variables had to be used. We used several model selection methods in SAS to identify potential models, and the final models were selected based on their parsimony, overall fit, stability of parameter estimates, adherence to model assumptions such as normality of the errors, and homoscedasticity (constant variance).

There was a strong correlation ($R^2 = 0.8630$) between the measured cell concentration and that predicted from a model based on the concentration of TOC, NH_4^+, and Ca^{2+}, and the fit of the model was improved ($R^2 = 0.9655$) when site was included as a class variable (Fig. S3). The relative importance of these variables can be determined by comparing P values from the parameter estimates, which indicated that TOC was the most significant ($P = 0.0053$) and Ca^+ ($P = 0.0517$) was the least significant variable for predicting cell concentration. At −7 °C, −6 °C, and −5 °C, there was a strong correlation (Fig. S3) between the abundance of biological ice nuclei and the concentration of Cl^-, SO_4^{2-}, and TOC, SO_4^{2-}, HCO_3^-, cells, and, NH_4^+, and NH_4^+, PO_4^{3-}, K^+, and Ca^{2+}, respectively, which are listed as variables of higher to lower significance based on their P value ranking.

Discussion

More than half of the rain and snow samples contained ice nuclei active at ≥ −5 °C, and all were active at temperatures warmer than −10 °C (Fig. 1). Based on their thermal sensitivity (Fig. 2), the vast majority (95%) of ice nuclei active at temperatures warmer than −10 °C are inferred to be proteinaceous, and therefore, biological in origin. There were samples where 100% of the ice nuclei at a given temperature were inactivated by lysozyme, which hydrolyzes the peptidoglycan backbone of bacterial cell walls, but on average, less than half (42%) were susceptible to digestion by this enzyme. If all bacteria in our samples were sensitive to lysozyme, then our results suggest that the majority of biological ice nuclei we analyzed originated from other sources (e.g., plants, fungi, and/or archaea). However, many bacteria are resistant to lysozyme and their susceptibility largely depends on the cells' physiological state (18). Hence, the fraction of ice nuclei we report as originating from bacteria should be viewed as a conservative estimate and deciphering the specific nature of these biological particles requires further experimentation.

Plant canopies and decaying vegetation are thought to represent significant terrestrial sources of atmospheric biological ice nuclei (8, 12, 19, 20), and consistent with this idea, the lowest concentrations of biological ice nuclei observed were in snow from Antarctica. The snow samples examined from Montana and France were collected during months when local deciduous plants were defoliated and leaf litter was buried beneath a seasonal snow pack. However, lower elevation plains and pasture lands in France and the western United States are snow-free and have exposed vegetation for much of the winter. Although coniferous vegetation existed near all of the sampling sites in Montana, previous studies have shown that these plant species harbor ice-nucleating bacteria at concentrations that are "very low or below detection" (12). Morris *et al.* (15) recovered pathogenic ice nucleating strains of *P. syringae* from 3 of the 7 snow samples we analyzed from France. Although we cannot determine what portion of the *P. syringae* cells in the snow were ice nucleating active at the time of deposition, these findings suggest that this phytopathogen may represent a significant fraction of the biological ice nuclei in precipitation at some locations and under certain environmental conditions.

Despite substantial differences in local ecosystems, sources of moisture, and air mass trajectory, the concentrations of ice nuclei active at ≥ −7 °C in midlatitude snow (3–150 ice nuclei L^{-1}) and Louisiana rain (8–230 ice nuclei L^{-1}) were remarkably similar (Fig. 1). These values are comparable to the range of ice nuclei concentrations reported in various rain samples from Alberta, Canada (≈20–600 ice nuclei L^{-1} based visually on data in figures 2 and 3 of ref. 21). The highest ice nuclei concentrations reported by Vali (21) corresponded to "the first period of high intensity rain," which were significantly higher than those observed for "continuous-type rain." Because we did not sample temporally, our data represent a running count of all ice nuclei deposited per total volume of material collected for each precipitation event. There were two rain samples (August 17 and October 4) that contained substantially higher concentrations of ice nuclei than all others analyzed (Fig. 1*B*). These highly active samples were collected during brief showers and are consistent

with the observations of Vali (21). This result may be caused by elevated concentrations of ice nuclei present in the troposphere where the precipitation formed or could be a consequence of atmospheric washout, whereby the airborne particles were concentrated in the small rain volumes collected during these transitory precipitation events.

Based on the known sources of aerosols in the atmosphere, it was reasonable to assume a priori that seasonal climatic and vegetation differences affect the distribution of biological and chemical species in the atmosphere. Therefore, statistical methods were used to elucidate seasonal relationships in the immersion freezing activity of biological ice nuclei and examine correlations between their concentration and the chemistry of the precipitation. We used cluster analysis to examine 7 months of Montana snow data, which revealed a seasonal pattern between snowfalls with respect to their ice-nucleating activities (Fig. 3). The ice-nucleating activity of snow collected in October and November appeared to have unique characteristics, and snows at each site from December to April were similar. One potential explanation for the seasonal grouping of observations relates to substantial vegetation changes in the northwest United States from fall to winter and winter to early spring. For example, fall harvest of cereal grains and subsequent growth of winter wheat may represent a source of airborne bacteria. Populations of plant epiphytic bacteria in the Pacific Northwest, including *P. syringae*, vary greatly seasonally, with numbers increasing because of rain and subsequent plant growth in the spring (22).

Factors influencing the concentration of biological particles in clouds and the atmosphere include the ecosystems that contribute the particles, local topography, climatic conditions, season, wet scavenging, and cloud water chemistry (1, 23–27). Multiple regression analysis of the physical, microbiological, and biogeochemical data produced relatively simple models that fit the observed data well. Although the Montana sampling sites were located only ≈80 km apart, when site was included as a variable, the fit of the model was substantially improved, which suggests that the airborne biological particle concentration and snow chemistry were not homogeneous between the sites, which is also supported by the significant variation observed in the concentration of all classes of ice nuclei in snow deposited on the same date at the two sites (December 29 and February 24; Fig. 2*A* and Fig. S1*A*) and cluster analysis (Fig. 3 and Fig. S2). Not surprisingly, differences in the history of the air masses from which the particles originated, heterogeneity in the chemical species distributed in the atmosphere, and/or local microclimatic factors appear to play an important role in the concentration of cells coprecipitated with snow.

There was a negative correlation between cell density and the concentration of NH_4^+ and TOC in Montana snowfall. Microbial activity in natural and agricultural soils is a source of NH_3 gas to the atmosphere, where it is subsequently converted to NH_4^+ (28, 29). Sources of atmospheric TOC include vegetation, soils, photochemical reactions, and the combustion of fossil fuels and biomass (30–32). Recently it has been shown that suitable conditions and nutrient concentrations exist in cloud water to support bacterial reproduction (33, 34). At 0 °C, Sattler *et al.* (33) estimate that bacterial biomass in cloud droplets could increase 20% per day. Although we do not know the physiological status of the microorganisms deposited in the snow or their metabolic capabilities under atmospheric conditions, heterotrophic growth via the assimilation of carbon and nitrogen provides one plausible explanation for our results given the negative regression relationship between both TOC and NH_4^+ and the cell concentration.

Known biological IN from bacteria, fungi, plants, lichens, and invertebrates catalyze ice formation at temperatures ranging from −2 to −7 °C (5), and even within a clonal bacterial population, different temperature classes of ice nuclei can simultaneously exist (35). The expression of ice nuclei has been shown to be tightly regulated by the nature of the carbon source, presence of nutrients (N, P, S, and Fe), and temperature (36). At each temperature modeled, nutrients such as NH_4^+, PO_4^{3-}, SO_4^{2-}, and TOC were identified as statistically significant predictors for the concentration of biological ice nuclei. This observation may be related to the fact that expression of the ice nucleation phenotype depends on certain environmental factors (36). Although some marine environments appear to be sources of atmospheric ice nuclei (13, 37), there was a negative correlation between Cl^- and the biological ice nuclei concentration at −7 °C, implying that marine aerosols were not a source of these particles in the Montana snow samples at this temperature and may have been a source of inhibition. There was a negative regression relationship between the concentration of K^+ and biological ice nuclei at −5 °C, and although there is a weak positive correlation between the concentration of K^+ and Cl^- ($R^2 = 0.4283$), the available information does not provide strong support for marine aerosols representing the main source of K^+. Ice-nucleation activity in several *Pseudomonas* species has been shown to be effected by low pH (38), and considering that the pH of the snow was ≈4.5, HCO_3^- could serve as a buffer in atmospheric water droplets, explaining its positive correlation with the concentration of biological ice nuclei at −6 °C. Because biological ice nuclei represent a portion of the total cells (estimated at <0.4%; ref. 14), an inverse correlation with the concentration of cells at −6 °C would appear counterintuitive. However, laboratory studies of *P. syringae* have shown that as few as 1 in 10^6 cells can be ice nucleation active at temperatures warmer than −8 °C (35), and as described above, regulation of the phenotype largely depends on nutrient availability. The positive correlation between the TOC, NH_4^+, Ca^{2+}, and biological ice nuclei concentration may be linked to known terrestrial sources of these aerosols (i.e., plant and soil ecosystems). The main source of atmospheric Ca^{2+} is soil-derived dust (29), and there was a positive correlation between the Ca^{2+} and the cell and biological ice nuclei concentrations at −5 °C. Soils have been shown to contain large concentrations of highly-active ice nuclei (39), and soil-derived particles transported through the atmosphere are likely to harbor assemblages of attached microorganisms (33). Elevated microbial cell concentrations have also been shown to be correlated with high dust content in ice cores (40, 41).

Conclusion

The cumulative concentration of biological ice nuclei active at temperatures warmer than −10 °C in precipitation collected from diverse worldwide locations ranged from 4 to 490 ice nuclei L^{-1} of rain or snow water equivalent. Based on their distribution in the atmosphere, biological ice nuclei are likely to encounter the appropriate conditions to affect atmospheric processes leading to precipitation. The meteorological role of biological ice nuclei could be particularly relevant at cloud temperatures that limit the action of other ice nuclei, but clearly, additional experimentation in atmospheric physics and modeling is required to assess their climatic importance. In addition to the potential role that cells may play in meteorological processes, microbiological studies of the atmosphere have broader implications for understanding the distribution and evolution of microbial life. Unlike animals, microorganisms are not geographically restricted and many species have been shown to occur globally (e.g., ref. 42); however, very little is known about modes of microbial dispersal on a planetary scale. The concept that biologically-catalyzed ice formation in the atmosphere could serve as a microbial dissemination strategy warrants more detailed investigation.

A key point regarding our data is that we infer that 95% of all ice nuclei active at temperatures warmer than −10 °C in snow

and rain were biological particles and >40% were confirmed to be bacterial in origin. However, the data available do not allow us to identify the specific nature of the majority of ice-nucleating biological particles that were detected. Statistical analysis revealed significant correlations between select biogeochemical variables and the cell and biological ice nuclei concentration in the precipitation. Based on the known sources of these aerosols and similarities between observations from the same season, our results lend support to the idea that terrestrial vegetation and soils are an important source of the biological ice nuclei distributed in the atmosphere. Although it is not possible to accurately back-calculate the abundance of ice nuclei in clouds based on concentrations in precipitation, our results imply that biological ice nuclei are widespread in the troposphere and underscore the need for quantitative data to gauge their influence on climate.

Materials and Methods

The particles >0.2 μm in precipitation samples were collected and reconstituted in deionized water followed by immersion freezing testing and successive treatment with lysozyme (3 mg mL^{-1}; 4 °C for 72 h) and heat (95 °C for 10 min). Profiles of freezing were generated at 1° increments between −2 °C and −13 °C for aliquots of this material and used to estimate the total, lysozyme-sensitive, and heat-sensitive cumulative IN concentration per volume of sample (14). Data from the Montana snow samples, together with concomitant measurements of the major ion (Metrohm Peak Ion Chromatograph), organic carbon (Dohrman DC80), cell, and particle (Microcyte flow cytometer) concentrations, were analyzed statistically with SAS (www.sas.com). Cluster and multiple regression analyses were used to examine similarity between freeze characteristics in individual precipitation events and identify the most significant predictors of the biological IN and cell concentration, respectively. Explicit detail on our methodology is provided in *SI Text*.

ACKNOWLEDGMENTS. We thank G. Vali and J. Geaghan for discussion, P. Amato and 2 anonymous reviewers for constructive comments on the manuscript and I. Bornard, M. Bardin, C. Glaux, F. Johnson, T. Leonard, S. Savage, and S. Trautman for collecting snow samples. This research was supported by a Louisiana State University Faculty Research grant (to B.C.C.), Montana State University–Vice President of Research and Yukon Geological Survey grants (to M.L.S.), National Science Foundation Grant OPP-0440943 (to C.M.F.), and the Institut National de la Recherche Agronomique's Department of Plant Health and Environment (C.E.M.).

1. Pruppacher HR, Klett JD (1997) *Microphysics of Clouds and Precipitation* (Kluwer, Dordrecht, The Netherlands), 2nd Ed.
2. Szyrmer W, Zawadzki I (1997) Biogenic and anthropogenic sources of ice-forming nuclei: A review. *Bull Am Meteor Soc* 78:209–228.
3. Vali G (1995) Principles of ice nucleation. *Biological Ice Nucleation and Its Applications*, eds Lee RE, Jr, Warren GJ, Gusta LV (APS Press, St. Paul).
4. Maki LR, Galyan EL, Chang-Chien M-M, Caldwell DR (1974) Ice nucleation induced by *Psuedomonas syringae*. *Appl Microbiol* 28:456–459.
5. Lundheim R (2002) Physiological and ecological significance of biological ice nucleators. *Philos Trans R Soc London* 357:937–943.
6. Sands DC, Langhans VE, Scharen AL, de Smet G (1982) The association between bacteria and rain and possible resultant meteorological implications. *J Hungarian Meteorol Serv* 86:148–152.
7. Amato P, *et al.* (2007) Microorganisms isolated from the water phase of tropospheric clouds at the Puy de Dôme: Major groups and growth abilities at low temperatures. *FEMS Microbiol Ecol* 59:242–254.
8. Lindemann J, Constantinidou HA, Barchet WR, Upper CD (1982) Plants as sources of airborne bacteria including ice nucleation-active bacteria. *Appl Environ Microbiol* 44:1059–1063.
9. Gurian-Sherman D, Lindow SE (1993) Bacterial ice nucleation: Significance and molecular basis. *FASEB J* 7:1338–1343.
10. Jayaweera K, Flanagan P (1982) Biogenic ice nuclei in the arctic atmosphere. *Geophys Res Lett* 9:94–97.
11. Morris CE, Kinkel LL (2002) in *Phyllosphere Microbiology*, eds Lindow SE, Hecht-Poinar EI, Elliot V (APS Press, Minneapolis), pp. 353–363.
12. Lindow SE, Arny DC, Upper CD (1978) Distribution of ice nucleation-active bacteria on plants in nature. *Appl Environ Microbiol* 36:831–838.
13. Schnell RC, Vali G (1975) Freezing nuclei in marine waters. *Tellus* 27:321–323.
14. Christner BC, Morris CE, Foreman CM, Cai R, Sands DC (2008) Ubiquity of biological ice nucleators in snowfall. *Science* 319:1214.
15. Morris CE, *et al.* (2008) The life history of the plant pathogen *Pseudomonas syringae* is linked to the water cycle. *ISME J* 2:321–334.
16. Constantinidou HA, Hirano SS, Baker LS, Upper CD (1990) Atmospheric dispersal of ice nucleation-active bacteria: The role of rain. *Phytopathology* 80:934–937.
17. Jaenicke R (2005) Abundance of cellular material and proteins in the atmosphere. *Science* 308:73.
18. Tolker-Nielsen T, Holmstrom K, Molin S (1997) Visualization of specific gene expression in individual *Salmonella typhimurium* cells by in situ PCR. *Appl Environ Microbiol* 63:4196–4203.
19. Schnell RC, Vali G (1972) Atmospheric ice nuclei from decomposing vegetation. *Nature* 236:163–165.
20. Schnell RC, Vali G (1973) Worldwide source of leaf-derived freezing nuclei. *Nature* 246:212–213.
21. Vali G (1971) Freezing nucleus content of hail and rain in Alberta. *J Appl Meteor* 10:73–78.
22. Caristi J, Sands DC, Georgakopoulos DG (1991) Simulation of epiphytic bacterial growth under field conditions. *Simulation* 56:295–301.
23. Lighthart B, Shaffer BT (1995) Airborne bacteria in the atmospheric surface layer: Temporal distribution above a grass seed field. *Appl Environ Microbiol* 61:1492–1496.
24. Giorgio CD, *et al.* (1996) Atmospheric pollution by airborne microorganisms in the city of Marseilles. *Atmos Environ* 30:155–160.
25. Fuzzi G, Mandrioli P, Perfetto A (1997) Fog droplets: An atmospheric source of secondary biological aerosol particles. *Atmos Environ* 31:287–290.
26. Marshall WA, Chalmers MO (1997) Airborne dispersal of Antarctic algae and cyanobacteria. *Ecography* 20:585–594.
27. Amato P, *et al.* (2007) An important oceanic source of microorganisms for cloud water at the Puy de Dôme (France). *Atmos Environ* 41:8253–8263.
28. Burns DA (2003) Atmospheric nitrogen deposition in the Rocky Mountains of Colorado and southern Wyoming: A review and new analysis of past study results. *Atmos Environ* 37:921–932.
29. Hidy GM (2003) Snowpack and precipitation chemistry at high altitudes. *Atmos Environ* 37:1231–1242.
30. Chebbi A, Carlier P (1996) Carboxylic acids in the troposphere, occurrence, sources, and sinks: A review. *Atmos Environ* 24:4233–4249.
31. Granby K, Christensen CS (1997) Urban and semirural observations of carboxylic acids and carbonyls. *Atmos Environ* 10:1403–1415.
32. Limbeck A, Puxbaum H (1999) Organic acids in continental background aerosols. *Atmos Environ* 33:1847–1852.
33. Sattler B, Puxbaum H, Psenner R (2001) Bacterial growth in supercooled cloud droplets. *Geophys Res Lett* 28:239–242.
34. Amato P, *et al.* (2007) A fate for organic acids, formaldehyde and methanol in cloud water: Their biotransformation by microorganisms. *Atmos Chem Phys* 7:4159–4169.
35. Fall R, Wolber PK (1995) Biochemistry of bacterial ice nuclei. *Biological Ice Nucleation and Its Applications*, eds Lee RE, Jr, Warren GJ, Gusta LV (APS Press, St. Paul, MN).
36. Nemecek-Marshall M, LaDuca R, Fall R (1993) High-level expression of ice nuclei in a *Pseudomonas syringae* strain is induced by nutrient limitation and low temperature. *J Bacteriol* 175:4062–4070.
37. Bigg EK (1973) Ice nucleus measurements in remote areas. *J Atmos Sci* 30:1153–1157.
38. Muryoi N, Kawahara H, Obata H (2003) Properties of a novel extracellular cell-free ice nuclei from ice-nucleating *Pseudomonas antarctica* IN-74. *Biosci Biotechnol Biochem* 67:1950–1958.
39. Upper CD, Vali G (1995) The discovery of bacterial ice nucleation and its role in the injury of plants by frost. *Biological Ice Nucleation and Its Applications*, eds Lee RE, Jr, Warren GJ, Gusta LV (APS Press, St. Paul, MN).
40. Abyzov SS, Mitskevich IN, Poglazova MN (1998) Microflora of the deep glacier horizons of central Antarctica. *Microbiology* (Moscow) 67:66–73.
41. Christner BC, *et al.* (2000) Recovery and identification of viable bacteria immured in glacial ice. *Icarus* 144:479–485.
42. Finlay BJ, Clarke KJ (1999) Ubiquitous dispersal of microbial species. *Nature* 400:828.

Supporting Information

Christner *et al.* 10.1073/pnas.0809816105

SI Text

Sampling and Site Locations. Snow was sampled from the vicinity of Bozeman, Montana at 4 ski resorts (Bridger Bowl, 45° 49′ 02″N, 110° 54′ 31″W; Big Sky Resort, 45° 16′ 12″N, 111° 17′ 59″W; The Yellowstone Club, 45° 15′ 39″N, 111° 24′ 45″W; and Moonlight Basin, 45° 17′ 29″N, 111° 26′ 13″W); at 5 sites in France in the Alps (La Clusaz, 45° 54′ 22″N, 06° 26′ 11″E, Villard de Lans, 45° 03′ 06″N, 05° 33′ 49″E, Saint-François Longchamp, 45° 24′ 36″N, 06° 20′ 53″E), the Pyrenees (Font Romeu, 42° 30′ 19″N, 02° 02′ 31″E), and in the Southeast (St. Saturnin-les-Avignon, 43° 57′ 34″N, 04° 55′ 22″E); in Antarctica (McMurdo Station, Ross Island, 77° 50′ 00″S, 166° 36′ 00″E); and from the Wheaton Glacier, 80km southwest of Whitehorse, Yukon (60° 04′ 00″N, 135° 34′ 00″W) from October 2005 to June 2006. Freshly fallen snow was collected aseptically as described (1).

Rain was collected from the roof of a 6-story building on the campus of Louisiana State University (Baton Rouge, 30° 24′ 40″N, 91° 10′ 38″W) from July to October 2007 by using sterile 35-cm-diameter polypropylene funnels (United States Plastic) and 2-L Erlenmeyer flasks. The collected rain was processed immediately or stored overnight in a sterile container at 4 °C, and all samples were analyzed <18 h after precipitation.

Immersion Freezing Testing and Determining the Ice Nuclei Concentration. At least 1 kg of fresh snow (melted at ≈4 °C over ≈18 h) or 80–500 ml of rain was used for determining the concentration of ice nuclei per unit volume. The particles >0.2 μM were collected by vacuum (25 kPa) filtration (Poretics; K02BP04700) and suspended in a volume of deionized H_2O that concentrated the particulates by a factor of 5- to 100-fold greater than that in the original snow or rain sample. The concentrated sample was aliquoted (0.25–1 ml) into 40–50 test tubes (1.5 ml) and the temperature at which aliquots of the concentrated sample froze was measured at 1° intervals from −2 °C to −13 °C in a polyethylene glycol bath (Thermo Electron; Neslab RTE-17). After freezing, samples were thawed, lysozyme (Fisher; BP535-5) was added to a final concentration of 3 mg·mL^{-1}, the mixture was incubated at 4 °C for 72 h, and the freezing profile was subsequently determined as described above. The remaining frozen tubes were thawed and heated to 95 °C for 10 min., followed by immersion freezing testing. Control samples that did not receive lysozyme or heat treatment were analyzed in parallel to confirm that the 2 freezing and thawing events did not significantly alter the original freezing profiles of the samples.

The total cumulative ice nuclei concentration (i.e., abiotic and biotic) at temperatures between −3 °C and −12°C was calculated by using equation **15** in the method described by Vali (2). The concentration of bacterial and biological ice nucleators (Fig. S1) was estimated by determining the fraction of ice nuclei that were susceptible to digestion with lysozyme and heat treatment, respectively, at each temperature interval.

Major Ion Chemistry. One-kilogram samples of snow were melted and filtered through a 0.2-μm filter for ion chemistry (Table S1). Aliquots of the filtrate were analyzed by using a Metrohm Peak Ion Chromatograph. Laboratory-prepared standards, certified standard solutions, and blanks were analyzed during all runs for quality assurance and control. The detection limit for major cations and anions was 5 ppb for Na^+, Cl^-, NO_2^-, NO_3^-, NH_4^+, and SO_4^{2-}, and 10 ppb for K^+, Ca^{2+}, Mg^{2+}, PO_4^{3-}, and the organic acid anions CH_3COO^- and $CHOO^-$. Precision, calculated as the coefficient of variation (100 s/x, where s is the standard deviation and x is the mean), for all major ions was <3%. Accuracy, calculated as the relative mean error with respect to known standards, ranged from <1% to 5% for all major cations and anions.

TOC. Samples for TOC were analyzed by using a photooxidative method. TOC is defined here as the dissolved and particulate organic carbon remaining in samples upon acidification to pH 2 with 20% H_3PO_4 and sparging with ultrapure oxygen for 6 min. The method relies upon oxidation via a combination of persulfate and UV radiation, followed by detection with a nondispersive infrared sensor (Dohrman DC80). All glassware used in the analysis were soaked overnight in 10% HCl followed by 6 rinses with nanopure water and 4 h of baking at 450 °C. Standards were mixed from potassium hydrogen phthalate in nanopure water, with analytical blanks consisting of acidified and sparged nanopure water. Four replicate injections were made of acidified and sparged samples and the average values are presented in Table S1.

Total Particle and Cell Concentration. A flow cytometer was used to characterize particles and DNA-containing cells in selected snow samples (Table S1). Measurements were performed with a Microcyte flow cytometer inside a class 100 clean hood, which was calibrated by using size and fluorescence intensity beads (Bangs Laboratories and Invitrogen). Samples were fixed with 5% formalin and stained at 37 °C with 5 μM SYTO 60 (Invitrogen) nucleic acid stain for 5 min in the dark. After incubation the samples were gently sonicated in a water bath and analyzed for 100 cycles with a 633-nm laser. Forward light scatter was used to measure the size and abundance of all particles, while fluorescence counts discriminated the biotic from the abiotic particles in the samples (Table S1).

Statistical Analyses. Cluster analysis (4) was used to classify the various Montana snowfall events into groups of similar snow events based on the probability of freezing between −2 °C and −9°C (Fig. S2). One problem with using the cumulative ice nuclei concentration for this analysis is that estimates of this quantity are unavailable at temperatures at which all sample tubes are frozen. On the other hand, estimated freeze probabilities are available in such situations. Because of this, the estimated freeze profiles from −2 °C to −9 °C were used in the cluster analysis. The proportion of frozen tubes at a given temperature (t °C) was used to estimate the probability of a tube being frozen at that temperature. These probabilities were provided as input to the clustering program that grouped snow samples with similar freeze profiles together. Similarities between observations were examined by using four hierarchical clustering methods: single linkage (minimum distance or nearest-neighbor distance), complete linkage (maximum distance or farthest-neighbor distance), average linkage (average distance of all pairwise inter-cluster distance), and Ward's method (Fig. S2).

Both the concentration of total cells and the concentration of biological ice nuclei were modeled as functions of several explanatory variables including major ion content (HCO_3^-, CH_3COO^-, Cl^-, NO_3^-, PO_4^{3-}, SO_4^{2-}, Na^+, NH_4^+, K^+, Ca^{2+}, Mg^{2+}), total dissolved solids, TOC, particle concentration, and cell concentration (when applicable). Site location was also considered as a class variable and used in some models. Models relating these response variables and the explanatory variables listed were created by using multiple regression analysis. Because

of the small sample size ($n = 10$) and the comparatively large number of explanatory variables ($P = 14$ or 15), forward selection model building procedures had to be used. The goal was to find parsimonious models that still fit the data well, without overfitting. Models were of the form:

$$Y = \beta_0 + \beta_1 X_1 + \beta_2 X_2 \ \ldots \ + \beta_k X_k + \varepsilon, \qquad [1]$$

where Y is the concentration being modeled, X_i is the ith explanatory variable in the model, β_i is the coefficient on the ith explanatory variable, ε is a random error term (assumed to be normally distributed), and k is the number of explanatory variables used in the model. Because of the large range and potential skewness for some parameters, the TOC, particle, and cell concentration data were logarithmically transformed. The concentration of formate and NO_2^- were below the instrumental level of detection for most samples (Table S1), so these data were excluded in model construction. Point estimates of the cumulative biological ice nuclei concentration were computed by using the formulas given in Vali (2), and confidence interval estimates were constructed by using the procedures presented by McCarter *et al.* (3).

SAS was used to build the models. There are several model selection options available in SAS . We used three to identify potential models: the SELECTION = RSQUARE, SELECTION = ADJRSQ, and SELECTION = MAXR methods. For each user-specified number of explanatory variables, the SELECTION = RSQUARE method fits all possible models and identifies those with the highest coefficient of determination (R^2), and lists them in decreasing order of R^2. The SELECTION = ADJRSQ method is similar, using the adjusted R^2 instead. The SELECTION = MAXR option is a forward selection technique that starts with the single variable model possessing the highest R^2, and then creates models involving an increasing number of variables, at each step adding the variable that results in the largest increase to R^2. At each step, a variable already in the model can be removed if replacing it by a variable not yet in the model would result in an increase in R^2. Each of these methods was used to identify potential models. The potential models were then compared and the final models were selected based on their parsimony, overall fit, stability of parameter estimates, adherence to model assumptions such as normality of the errors, and homoscedasticity (constant variance). The REG procedure was used to fit the models and to calculate various model diagnostics. The UNIVARIATE procedure was used to formally test for violations of the normality assumption, and residual plots were used to visually check for violations of the constant variance assumption.

Using the concentration of fluorescently-labeled DNA-containing cells L^{-1} (Table S1) as the response variable, the model was simplified to the three most significant variables, which were the concentrations of TOC, NH_4^+, and Ca^{2+}. The regression equation derived for the model, designated cell model 1, was:

$$\text{Cells } L^{-1} = \exp(13.4 - 0.350*\ln[\text{TOC}] - 0.107*[NH_4^+] + 0.314*[Ca^{2+}]). \qquad [2]$$

Three of the four Montana snow collection sites (BS, YC, and MB) are in close proximity and were designated as a single site. A variation on cell model 1 incorporated the site location as a class variable (i.e., value of 0 for the BB site and 1 for the BS, YC, and MB sites). The equation for the revised model (cell model 2) including site was:

$$\text{Cells } L^{-1} = \exp(12.9 - 0.329*\ln[\text{TOC}] - 0.066*[NH_4^+] + 0.262*[Ca^{2+}] + 0.625*[\text{Site}]). \qquad [3]$$

There was a strong correlation between the predicted and observed cell concentration values (Fig. S3) for cell model 1 ($R^2 = 0.8630$), and the correlation improved ($R^2 = 0.9655$) when site location was included in the model (cell model 2).

We point out that the biological ice nuclei concentrations do exist in our data for all snow events at −5 °C. However, several of these concentrations are 0, because for some samples no tubes were frozen at −5 °C. Because of this, we also modeled the concentration at −6 °C and −7 °C because there were at least some tubes frozen in all samples at these temperatures. However, at both −6 °C and −7 °C, there were one or more snow events for which the biological ice nuclei concentrations could not be calculated because all sample tubes were frozen at these temperatures (calculation of the cumulative concentration requires that at least one tube not be frozen). To perform the regression analyses at these temperatures, missing concentrations either had to be left out of the analyses or be imputed. Several approaches were considered. The first approach replaced a missing concentration at −7 °C with the concentration from the coldest temperature above −7 °C when the concentration could be calculated. The second imputation procedure replaced a concentration missing at −6 °C with the concentration at −5 °C. We also fit a model using only those snow events possessing non-missing concentrations at −6 °C (only 1 sample had a missing cumulative concentration at −6°C, BB, February 24). Finally, we fit a model using the concentrations at −5 °C.

The biological ice nuclei concentration was modeled as a function of several explanatory variables separately at temperatures −7 °C, −6 °C, and −5 °C (Fig. S3). Unlike models constructed to fit the cell concentration data, the inclusion of site as a variable did not appreciably increase the fit of the models. In modeling the biological ice nuclei concentration at −7 °C, the RSQUARE method identified the model containing the explanatory variables Cl^-, SO_4^{2-}, K^+, and TOC as the best four-variable model, and the model containing Cl^-, SO_4^{2-}, and TOC as the best 3-variable model. In addition, the ADJRSQ method identified these as the top 2 models. After evaluating various fit statistics and checking for violations of model assumptions, the 3-variable model was selected as the final model. The fitted model (−7 °C biological ice nuclei model) is given by:

$$\text{Biological ice nuclei } L^{-1} = -80.17 - 12.07*[Cl^-] + 614.46*[SO_4^{2-}] + 18.04*\ln[\text{TOC}]. \qquad [4]$$

This model has a $R^2 = 0.8556$ (adjusted $R^2 = 0.7825$) and fits reasonably well. However, one of the imputed data points (YC, December 29) had a fairly large residual that adversely affected the fit and led to the plausibility that the errors were not normally distributed. When this observation was removed and the model refit, the normality assumption became much more plausible, and the model parameters did not change appreciably. Because the estimates are not largely affected when the observation is included, the original fitted model was chosen to describe the relationship between the biological ice nuclei concentration and the explanatory variables at −7 °C. Qualitatively, this model indicates that the biological ice nuclei concentration at −7 °C decreases as Cl^- increases and increases with an increase in either SO_4^{2-} or TOC.

In modeling the biological ice nuclei concentration at −6 °C, both the RSQUARE and the ADJRSQ methods identified the model containing the variables HCO_3^-, SO_4^{2-}, NH_4^+, and cell concentration as the best 4-variable model. The fitted model (−6 °C biological ice nuclei model) is given by:

$$\text{Biological ice nuclei } L^{-1} = 115.33 + 129.34*[HCO_3^-] + 177.48*[SO_4^{2-}] + 1.62*[NH_4^+] - 11.30*\ \ln[\text{Total Cells}]. \quad [5]$$

The model fits very well, having an adjusted R^2 of 0.9552 (R^2 = 0.9753). The normality assumption is reasonable based on formal tests ($P > 0.15$) and the diagnostic residual normal probability plot. According to this model, the biological ice nuclei concentration at −6 °C increases as HCO_3^-, SO_4^{2-}, or NH_4^+ increase, and it decreases as the cell concentration becomes larger.

Finally, in modeling the biological ice nuclei concentration at −5 °C, both the RSQUARE and ADJRSQ methods identified the model containing the variables PO_4^{3-}, NH_4^+, K^+, and Ca^{2+} as the best 4-variable model. The fitted model (−5 °C biological ice nuclei model) is given by:

$$\text{Biological ice nuclei } L^{-1} = 2.48 - 8.50*[PO_4^{3-}] + 4.57*[NH_4^+] - 29.15*[K^+] + 18.56*[Ca^{2+}]. \quad [6]$$

The model fits very well, possessing an adjusted R^2 of 0.9847 (R^2 = 0.9915). The normality assumption is reasonable based on formal tests ($P > 0.15$) and the diagnostic residual normal probability plot. According to this model, an increase in either PO_4^{3-} or K^+ is associated with a decrease in the biological ice nuclei concentration at −5 °C, whereas an increase in either NH_4^+ or Ca^{2+} is associated with an increase in the biological ice nuclei concentration.

1. Christner BC, Morris CE, Foreman CM, Cai R, Sands DC (2008) Ubiquity of biological ice nucleators in snowfall. *Science* 319:1214.
2. Vali G (1971) Quantitative evaluation of experimental results on the heterogenous freezing nucleation of supercooled liquids. *J Atmos Sci* 28:402–409.
3. McCarter KS, Cai R, Christner BC. Using generalized linear mixed models analysis for the detection and classification of biological ice nucleators. Applied Statistics in Agriculture Conference, April 29, 2008, Manhattan, KS.
4. Gan G, Ma C, Wu J (2007) *Data Clustering: Theory, Algorithms, and Applications.* (ASA, Alexandria, VA), ASA-SIAM Series on Statistics and Applied Probability, pp 107–150.

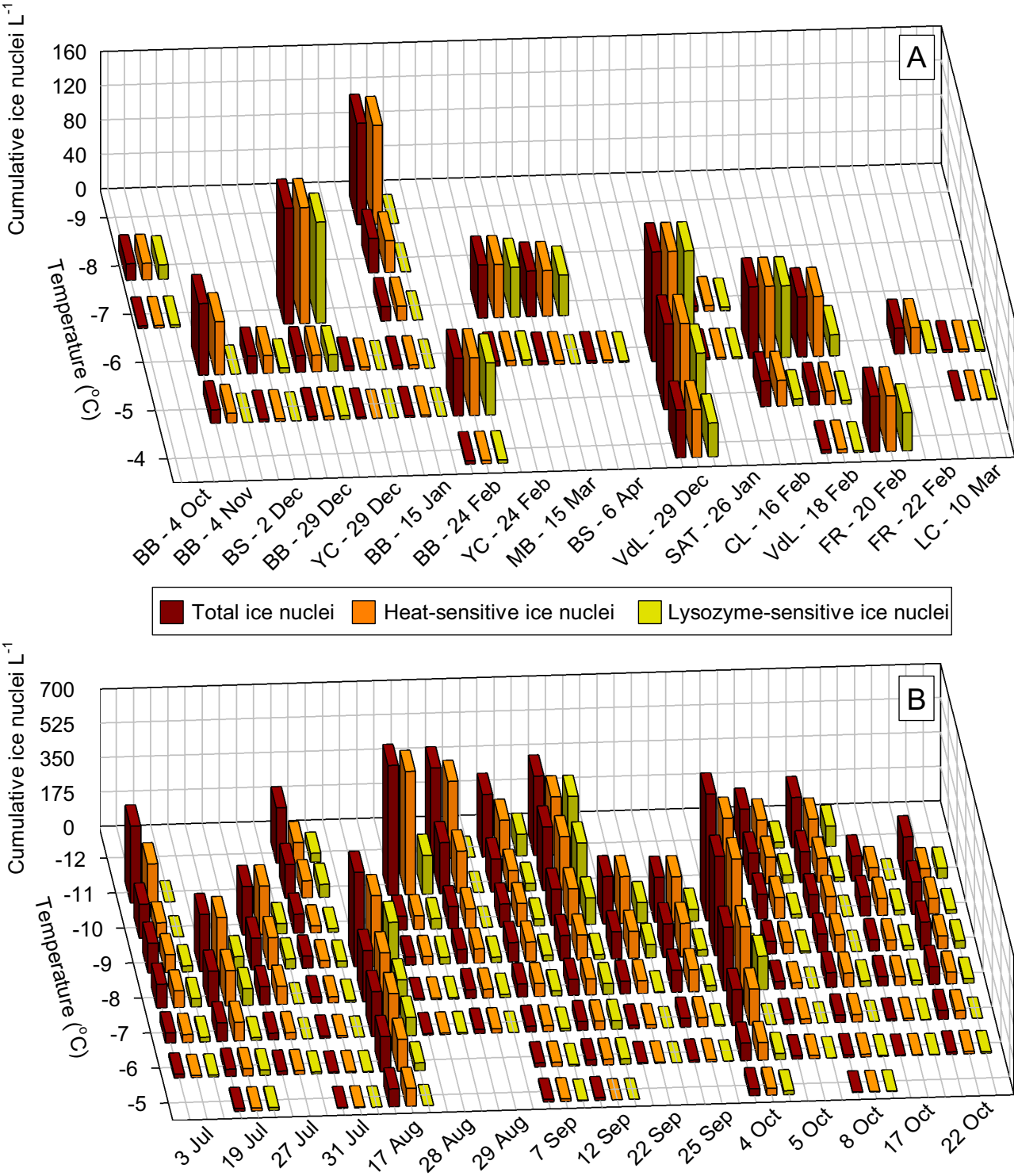

Fig. S1. The concentrations of total, biological, and bacterial ice nuclei at decreasing temperature. The concentration of biological and bacterial ice nuclei is based on the fraction that were susceptible to heat treatment and lysozyme digestion, respectively. (*A*) Snow from Montana and France. (*B*) Rain from Louisiana. See Fig. 1 legend for the site designations used.

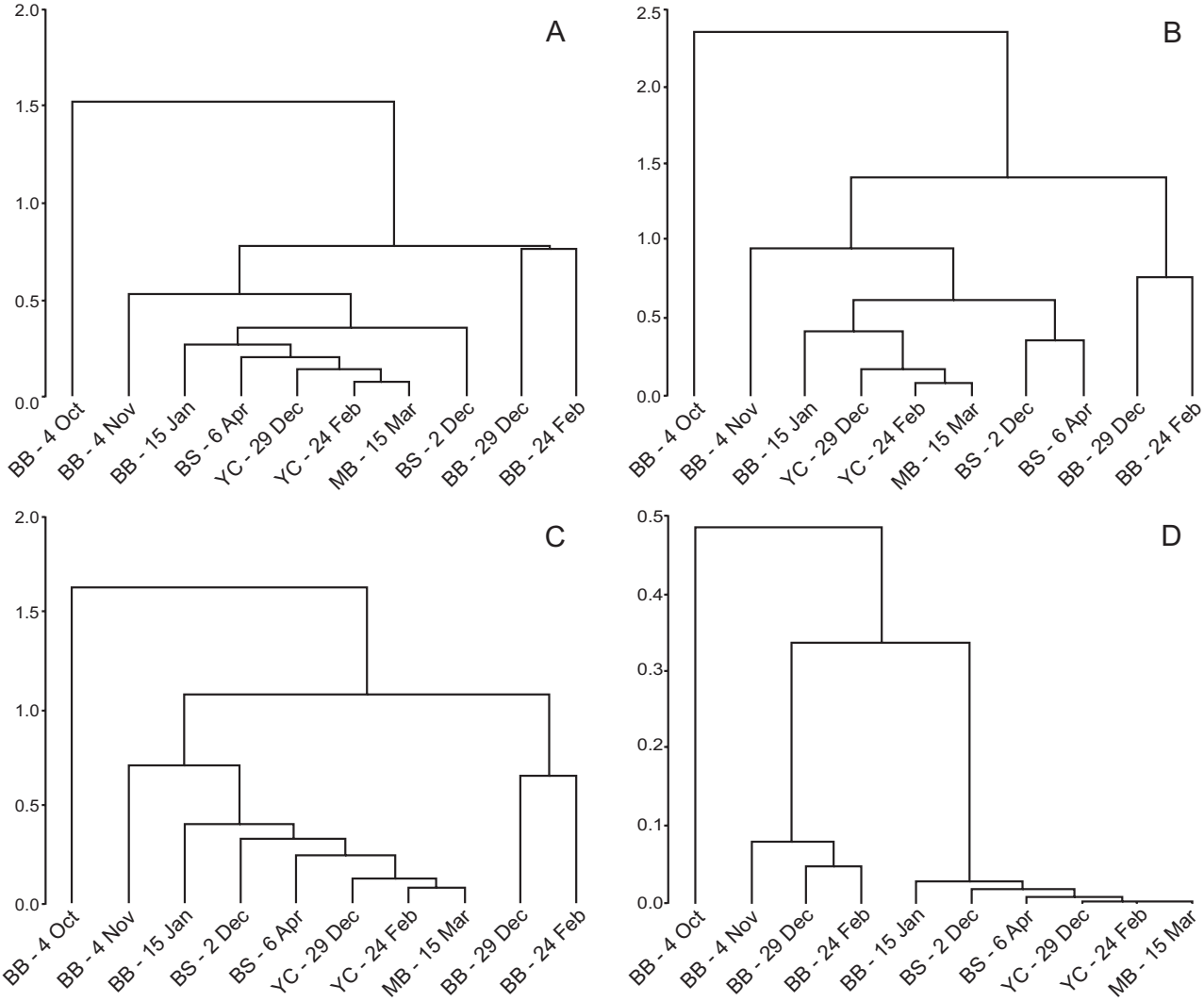

Fig. S2. Cluster analysis of Montana snowfall by single linkage (*A*), complete linkage (*B*), average linkage (*C*), and the Ward's method (*D*). In *A–C*, the scale bar indicates the maximum distance between clusters, and in *D*, it represents the semipartial R^2 values. Each sample is designated by the date of precipitation and the site of collection (see Fig. 1 legend for site designations).

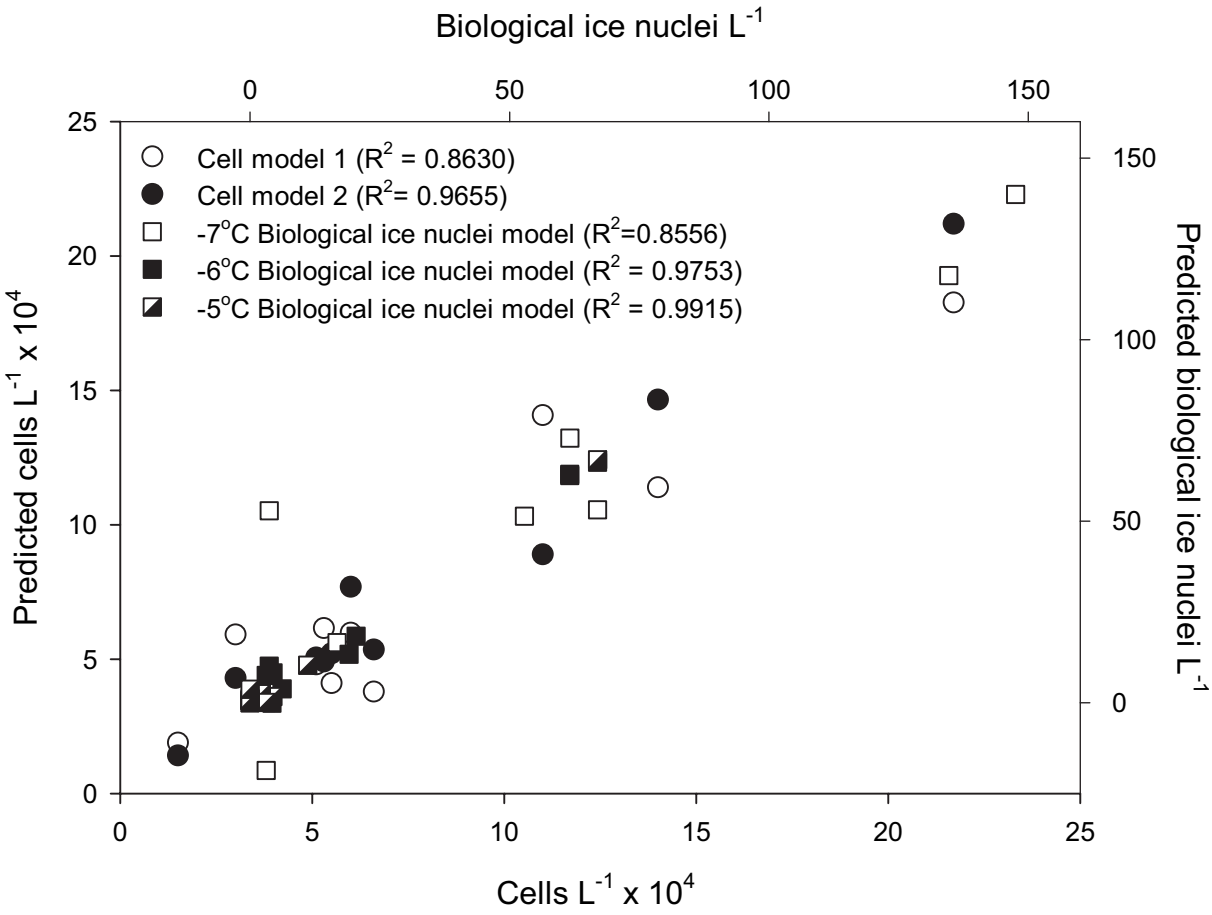

Fig. S3. Multiple scatter plot of the measured versus predicted data from multiple regression models for cell and biological ice nuclei concentration in snowfall samples deposited near Bozeman, Montana from October 2005 to April 2006. Cell concentrations are plotted against the lower *x* axis and left *y* axis; biological ice nuclei are plotted against the upper *x* axis and right *y* axis.

Table S1. Major ion, TOC, particle, and cell concentrations in snow samples from Montana

	μmol L^{-1}														Per L	
Site, date	CH_3COO^-	$HCOO^-$	Cl^-	NO_2^-	NO_3^-	PO_4^{3-}	SO_4^{2-}	HCO_3^-	Na^+	NH_4^+	K^+	Ca^{2+}	Mg^{2+}	TOC ($\times 10^2$)	Particles ($\times 10^7$)	Cells ($\times 10^4$)
BB, Oct. 4	0.37	BD	1.10	BD	0.84	0.34	BD	0.12	BD	0.36	0.83	1.20	0.30	2.2	1.1	11.0
BB, Nov. 4	3.70	BD	2.30	BD	5.90	7.20	0.14	0.18	BD	14.00	0.87	1.70	0.27	1.3	3.0	5.1
BS, Dec. 2	0.17	BD	0.76	BD	3.10	1.70	0.23	BD	0.26	0.72	0.77	1.70	0.02	1.4	4.6	22.0
BB, Dec. 29	BD	BD	BD	BD	1.70	0.24	0.03	BD	BD	0.69	0.06	BD	BD	200	1.5	1.5
YC, Dec. 29	0.86	BD	7.30	BD	1.60	0.88	0.10	BD	1.10	0.31	0.63	1.20	0.27	74	1.6	5.5
BB, Jan. 15	1.90	0.044	3.70	BD	2.10	0.95	0.03	BD	0.37	2.40	0.56	0.74	BD	8.9	1.7	3.0
BB - Feb. 24	9.30	BD	9.20	BD	3.30	3.80	0.16	0.24	BD	9.00	1.10	4.70	0.52	37	2.8	5.3
YC, Feb. 24	2.90	0.022	0.62	BD	1.80	4.50	0.09	0.01	BD	3.10	0.42	1.90	BD	3	1.4	14.0
MB, March 15	2.00	BD	2.40	BD	2.90	1.40	0.03	BD	0.13	2.70	0.37	0.63	0.24	26	2.1	6.6
BS, April 6	1.30	BD	11.00	BD	3.30	2.40	0.07	BD	1.90	2.20	1.10	2.20	0.26	33	1.1	6.0
Average	2.20	ND	3.80	ND	2.70	2.30	0.09	ND	0.37	3.50	0.67	1.60	0.19	39	2.1	8.0
Clancy, MT, fall 2005*	ND	ND	1.10	ND	7.40	ND	2.50	ND	1.20	7.80	0.56	2.70	0.49	ND	ND	ND
Clancy, MT, winter 2005*	ND	ND	0.56	ND	9.40	ND	1.60	ND	0.43	2.20	0.20	1.50	0.29	ND	ND	ND
Clancy, MT, winter 2006*	ND	ND	0.71	ND	5.00	ND	0.91	ND	0.48	2.10	0.46	1.80	0.33	ND	ND	ND
Clancy, MT, spring 2006*	ND	ND	0.73	ND	6.20	ND	2.10	ND	0.65	6.80	0.20	2.10	0.37	ND	ND	ND
YNP, WY, fall 2005*	ND	ND	2.00	ND	6.90	ND	2.80	ND	1.70	6.70	0.33	2.70	0.49	ND	ND	ND
YNP, WY, winter 2005*	ND	ND	0.28	ND	5.00	ND	1.00	ND	0.22	3.30	0.13	0.50	0.08	ND	ND	ND
YNP, WY, winter 2006*	ND	ND	1.10	ND	5.20	ND	1.40	ND	1.30	3.90	0.20	2.00	0.29	ND	ND	ND
YNP, WY, spring 2006*	ND	ND	4.30	ND	9.80	ND	6.50	ND	8.40	13.00	0.61	8.90	2.10	ND	ND	ND

*Precipitation-weighted mean ion concentration data from the National Atmospheric Deposition Program (http://nadp.sws.uiuc.edu/).

Data are from sites in Clancy, Montana and Yellowstone National Park (Tower Falls), Wyoming. The summary periods were from August 30 to December 29, 2005 for fall, from December 29, 2005 to February 28, 2006 for winter, and from February 28 to May 30, 2006 for spring. BD = species was at a concentration below detection limits of the instrument; ND = not determined.